Bioresource Technology Reports 34 (2026) 102676

Contents lists available at ScienceDirect

Bioresource Technology Reports

journal homepage: www.sciencedirect.com/journal/bioresource-technology-reports

Synthetic approach for the oxidative depolymerization of biomass-derived lignin to vanillin, vanillic acid, and acetovanillone compounds

Rohit Bains [a,b], Mahender Kumar [a,b], Arvind Singh Chauhan [a,b], Ajay Kumar [a,b], Pralay Das [a,b,*]

[a] Chemical Technology Division, CSIR-Institute of Himalayan Bioresource Technology, Palampur, 176061, H.P., India
[b] Academy of Scientific and Innovative Research (AcSIR), Ghaziabad, 201002, India

ARTICLE INFO

Keywords:
Kraft lignin
Biomass-derived lignin
Oxidative depolymerization
Phenolic compounds

ABSTRACT

A simple protocol has been developed for alkaline oxidative depolymerization of commercially available kraft lignin and biomass-derived lignin from bamboo, lemon grass, pine needles, and rice straw for the synthesis of phenolic compounds in a single pot under a hydrothermal reactor system. Herein, first time, we have demonstrated the effective oxidative reagent system MnO_2 and $Na_2H_3CO_6$ for the fractionation of lignin to vanillin, vanillic acid, and acetovanillone with 3.5–10, 3–6.5, and 1–1.5 wt% total yields, respectively. In addition, the morphological variations, particle size distribution and functional characteristics of different lignin substrates were characterized by SEM and FTIR analysis methods. The heterogeneous MnO_2 was easily recyclable up to five cycles, and the characterization of fresh and reactivated MnO_2 was analyzed through the XPS technique.

1. Introduction

In recent decades, the continuous depletion of fossil fuel resources and some major shortcomings in terms of its sustainability and long-term availability have encouraged the modern scientific community to focus on renewable sources for energy and chemical production. In this perspective, lignocellulosic biomass is naturally abundant, inexpensive, and sustainable, making it a promising alternative to bio-based aromatic compounds and fuels (Banu et al., 2021). Cellulose and hemicellulose are polymeric carbohydrate constituents of biomass and can be valorized to furan-based value-added compounds, whereas lignin is a complex amorphous non-carbohydrate component of the secondary cellular wall of plants (Kumar et al., 2023). After cellulose, lignin is the second-most bio-polymer (20–40 wt%) component of lignocellulosic biomass and has great potential for the development of various commercial phenolic compounds such as phenols, syringol, guaiacols, catechols, etc., having wide applications in pharmaceutical products, resin, food additives, bio-preservatives, and active ingredients of bio-jet fuel (Sun et al., 2018; Li et al., 2015).

Lignin is a naturally available aromatic polymeric feedstock with numerous phenolic properties. Every year, 50–70 million tonnes of lignin are produced as a by-product from the paper and pulp industries through the kraft pulping process and is known as kraft lignin (sulfur-containing lignin) (Bajwa et al., 2019). Nowadays, most of the lignin has been burned to obtain low-grade fuel, and only 5% is successfully utilized to value-added chemicals and materials synthesis through reductive, oxidative, and acid- or base-catalyzed depolymerization processes (Cao et al., 2019; Bu et al., 2012; Gillet et al., 2017). However, low reactivity, solubility, poor yields of products, and harsh reaction conditions are major problems for the bio-refinery of lignin. Despite all these hurdles, modern scientific communities are still focusing on finding solutions for the direct utilization of lignin to various phenolic compounds.

The oxidative depolymerization of lignin to vanillin, vanillic acid, and acetovanillone has recently been seen as the most promising technique performed under mild reaction conditions. Vanillin is a key molecule extensively employed as a fragrance and flavoring ingredient in the food and beverage industries, and is a primary component of the extract of vanilla beans (Pacek et al., 2013). Although the production of vanillin is less than 1% from vanilla beans, so the majority of vanillin is currently produced through petroleum-derived guaiacol (Fache et al., 2015). However, high price, low productivity, and the rising demand for vanillin to enhance the flavor/ aroma of the product are main growth factors. Thus, as compared to guaiacol, lignin is a more streamlined, economical, and highly abundant feedstock for vanillin production. Moreover, the global vanillin market is expected to grow from USD

* Corresponding author at: Chemical Technology Division, CSIR-Institute of Himalayan Bioresource Technology, Council of Scientific & Industrial Research, PO Box 06, Palampur, 176061, H.P., India.
E-mail address: pdas@ihbt.res.in (P. Das).

https://doi.org/10.1016/j.biteb.2026.102676
Received 12 December 2025; Received in revised form 25 February 2026; Accepted 26 February 2026
Available online 5 March 2026

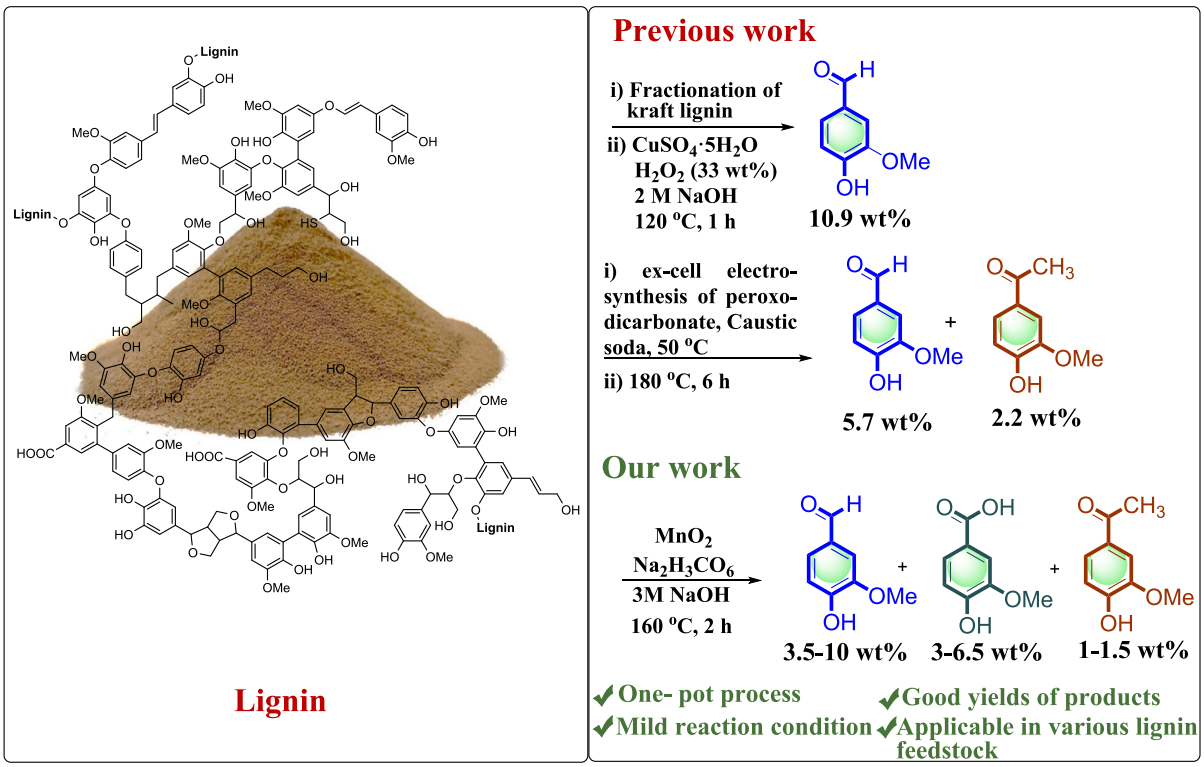

Scheme 1. Comparison of previous strategies with the present protocol.

958.57 million in 2023 to USD 1416.95 million by 2028, at a CAGR of 8.13% during the forecast period (2023–2028). In addition, vanillic acid is well known as a flavoring agent and also has a nutraceutical and therapeutic potential role, whereas acetovanillone (also known as apocynin) has effective pharmacological properties for diseases such as arthritis, atherosclerosis, and asthma (Kaur et al., 2022; Stefanska and Pawliczak, 2008). Therefore, several research communities are actively engaged in developing more efficient, scalable, selective, and one-pot processes for the production of such phenolic compounds from biomass-derived lignin.

Several approaches such as biochemical, reductive, thermal, and oxidative treatment, have been widely used for the depolymerization of lignin into various phenolic compounds. Voitl and Roh (2010) reported the oxidative depolymerization of industrial kraft lignin to vanillin and methyl vanillate, achieving 3.5 wt% yield for each product using an $H_3PMo_{12}O_{40}$ catalyst in an 80% methanol- 20% water solvent system at 170 °C and 10 bar O_2 for 20 min in a batch reactor (Voitl and Roh, 2010). During the journey for lignin depolymerization, Liu and co-workers reported the depolymerization of kraft lignin to vanillin with 5.3 wt% GC yield using molecular O_2 of 2.2 atm pressure at 197 °C for 2.4 h under a pressurized reactor system (Liu et al., 2020). Similarly, Zhang et al. reported a two-step synthesis of vanillin (10.9 wt%) through fractionation of kraft lignin utilizing 1-propanal alcoholic solvent under reflux conditions for 4 h and further fractionating part of lignin treated with $CuSO_4{\cdot}5H_2O$ catalyst and H_2O_2 as an oxidant in 2 M NaOH at 120 °C for 1 h (Zhang et al., 2020). Later on in the year 2021, the combining catalytic system $VO(acac)_2$-$Cu(OAc)_2$ was employed for the oxidative depolymerization of lignin to vanillin, vanillic acid, and acetovanillone with a total yield of 7 wt% under 2 M NaOH solution and 5 bar oxygen partial pressure at 150 °C for 45 min (Walch et al., 2021). Moreover, Zirbes et al. published a method for the selective degradation of kraft lignin into vanillin with yield up to 6.2 wt% using a peroxodicarbonate oxidant at 180 °C for 6 h (Scheme 1.) (Zirbes et al., 2023). Furthermore, cornstalk, beech, mixed hardwood, cedar lignin, and bamboo lignin were also employed for the synthesis of phenolic compounds (Deng et al., 2009; Stark et al., 2010; Liu et al., 2013; Yamamoto et al., 2017; Harshvardhan et al., 2017). However, the use of specially designed reactor systems, challenging separation of catalytic species, limited catalyst recyclability, and poor yield remains a big challenge for efficiently converting lignin to targeted compounds.

In this study, we developed a novel, one-step procedure for converting five major lignin types (kraft lignin, bamboo lignin, lemon grass lignin, pine needle lignin, and rice straw lignin) to phenolic compounds by utilizing commercially available manganese dioxide (MnO_2), in combination with sodium percarbonate ($Na_2H_3CO_6$) as a stable solid oxidant, under hydrothermal conditions. The combined MnO_2 and $Na_2H_3CO_6$ system operates without the need for expensive noble metals delivers enhanced selectivity toward high-value phenolic products such as vanillin, vanillic acid, and acetovanillone at 160 °C and 2 h reaction time using 3 M NaOH solvent media. Furthermore, this work systematically evaluates catalyst recyclability over multiple cycles, and the characterization of fresh and reactivated MnO_2 was analyzed through the XPS technique. In addition, the morphological variations, particle size distribution, and the functional characteristics of lignin feedstock were characterized by SEM and FTIR analysis methods, and also discusses the plausible reaction mechanism for lignin depolymerization.

2. Experimental section

2.1. Materials

Kraft lignin (~5% moisture), DMSO-d_6 (99.9%), Iron oxide (Fe_2O_3; ~99%), Zinc oxide (ZnO; ~99.9%), Dichloromethane (DCM; ≥99.9%), and sodium percarbonate ($Na_2H_3CO_6$; ~20–30% by weight H_2O_2) were purchased from Sigma-Aldrich. Hydrogen peroxide (H_2O_2; ~30% H_2O_2 by weight), Sodium sulfate (Na_2SO_4; ~99.50%), Sulphuric acid (H_2SO_4; ~98% H_2SO_4 by weight), Sodium hydroxide (NaOH; ≥ 98.0%), Cuprous oxide (CuO; *99.0%*), and Acetonitrile (ACN; 99.80%) were bought from SD Fine-Chem. Ltd. (SDFCL). Ethyl acetate (~99%), Hexane (~95%), and Hydrochloric acid (HCl; 35–38% by weight) were received from

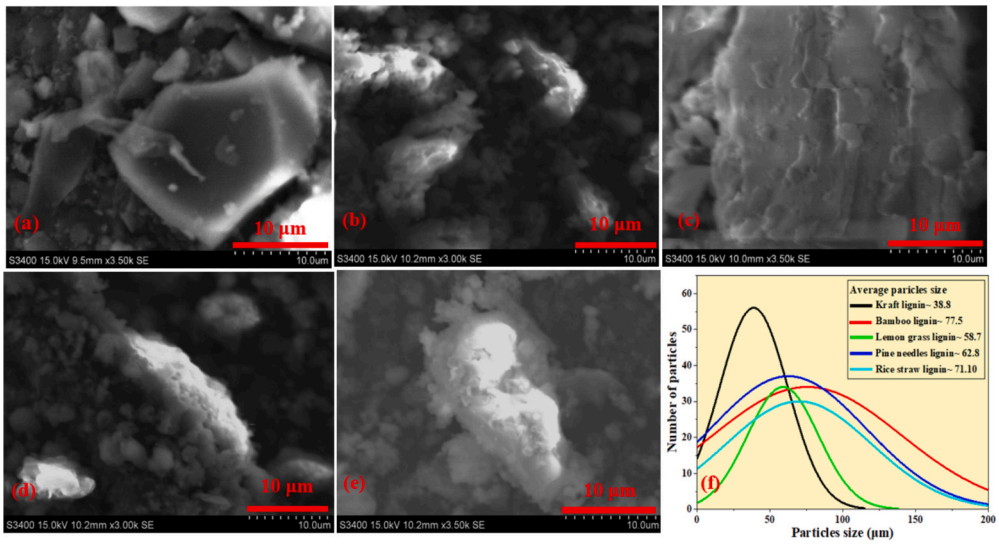

Fig. 1. SEM images of a) kraft lignin b) bamboo lignin c) lemon grass lignin d) pine needles lignin e) rice straw lignin at 10 µm scale and f) lignin particle size distribution.

Central Drug House (P) Ltd. Manganese oxide (MnO_2; 80%) was procured from Avra Synthesis (P) Ltd. All other four lignin such as bamboo lignin, lemon grass lignin, pine needles lignin, and rice straw lignin, were derived from their raw biomass by following particular literature reports (see ESI for more information) and used directly in reaction conditions without further purifications.

2.2. Instruments and measurements

The Jeol 500/400 MHz (^{1}H) and 150/100 MHz (^{13}C) Nuclear Magnetic Resonance (NMR) spectrometer was used for recording ^{1}H and ^{13}C NMR spectra for all synthesized compounds. The spectra of synthesized molecules were recorded at 25 °C under a DMSO-d_6 solvent system. The chemical shifts were recorded in δ (ppm) relative to the TMS and NMR solvent signal. The coupling constants (J) were given in Hz, and multiplicities were reported as s, singlet; d, doublet; m, multiplet. The mass spectrum of prepared compounds was performed on a Waters micro mass Q-TOF Ultima spectrometer and Agilent high-resolution Ion Mobility Q-TOF LC/MS spectrometer using electron spray ionization (ESI) technique. The morphological characterization of lignin substrates was analyzed through a Scanning Electron Microscope (SEM; Hitachi S-3400 N, Japan). The characteristics functional groups of various lignin were scrutinized by Fourier Transform Infrared Spectroscopy (FTIR; Shimadzu) in the range between 4000 and 400 cm^{-1}. On the same note, the oxidation state of iron (Mn) in MnO_2 of fresh and after reactivation was investigated through X-ray photoelectron spectroscopy (XPS; Thermofisher scientific, Nexsa base,). The UV/ Vis spectra of lignin were analyzed via Thermo Scientific GENESYS Spectrophotometers. In addition, thermogravimetric analysis (TGA) was performed using a PerkinElmer, and pore area analysis was conducted by Smart Instruments Co. Pvt. Ltd.

2.3. Procedure for the conversion of lignin to phenolic compounds

The oxidative depolymerization reactions of lignin were conducted in a stainless steel (SS 316) hydrothermal reactor with an inner Teflon vial having a 30 mL internal capacity. The inner Teflon vial was charged with lignin (200 mg), followed by the addition of MnO_2 (200 mg, 1 equiv. (w/w)) and $Na_2H_3CO_6$ (600 mg, 3 equiv. (w/w)). The reaction mixture was solvated with 3 M NaOH (10 mL) alkaline solvent media, and then Teflon vial was placed in a hydrothermal steel vial and screw tightened. The hydrothermal steel vial was placed on a heating stir and allowed to stir at 600 rpm at 160 °C for 2 h. Upon completion of the reaction, the hydrothermal reactor was cooled to room temperature, and the MnO_2 was filtered through a simple filtration method. The filtrate was neutralized with 4 N H_2SO_4 (10 mL), resulting in the formation of a precipitate of lignin fraction. The precipitate was filtered out, washed with ethanol, and dried. After that, the filtrate was extracted via ethyl acetate (3 × 10 mL) in frequent iterations, dried over anhydrous Na_2SO_4, and concentrated under reduced pressure through a rotary evaporator. Finally, the reaction mixture was purified through silica gel chromatography using hexane: ethyl acetate (95–85: 5–15) eluent for the procurement of desired phenolic compounds. The precipitated lignin was also applied under optimized conditions to further enhance the yields of desired products.

3. Results and discussion

Over the past few years, our research group has been constantly working on the valorization of lignocellulosic biomass to 5-HMF and furfural, and further their applications in the synthesis of valuable furan-based compounds (Bains et al., 2022; Bains et al., 2024). In continuing this research, herein, we have developed a new protocol for the oxidative depolymerization of various biomass-derived lignin to phenolic compounds such as vanillin, vanillic acid, and acetovanillone under hydrothermal reaction conditions. Moreover, the comprehensive characterizations, such as scanning electron microscopy and Fourier transform infrared analysis of lignin were briefly discussed.

3.1. Morphological and functional characterization of lignin

In order to determine the morphological characterization of lignin, we have performed SEM analysis of commercially available kraft lignin and other biomass-derived lignin. As shown in Fig. 1, all five lignins have different morphologies with small and large-sized pores as depicted at 10 µm. The kraft and lemon grass lignin have smooth surface characteristics with different particle sizes. However, the remaining lignin feedstock exhibited an amorphous fractured morphology of particles. Thus, the morphological variations in different lignin feedstocks might influence the yields of desired products. In addition, we have also determined the lignin particle size and noticed that each lignin feedstock had an inequitable size and shape. The predicted average particle size of kraft lignin, bamboo lignin, lemon grass lignin, pine needles lignin, and rice straw lignin were 38.8, 77.5, 58.7, 62.8, and 71.10 µm respectively.

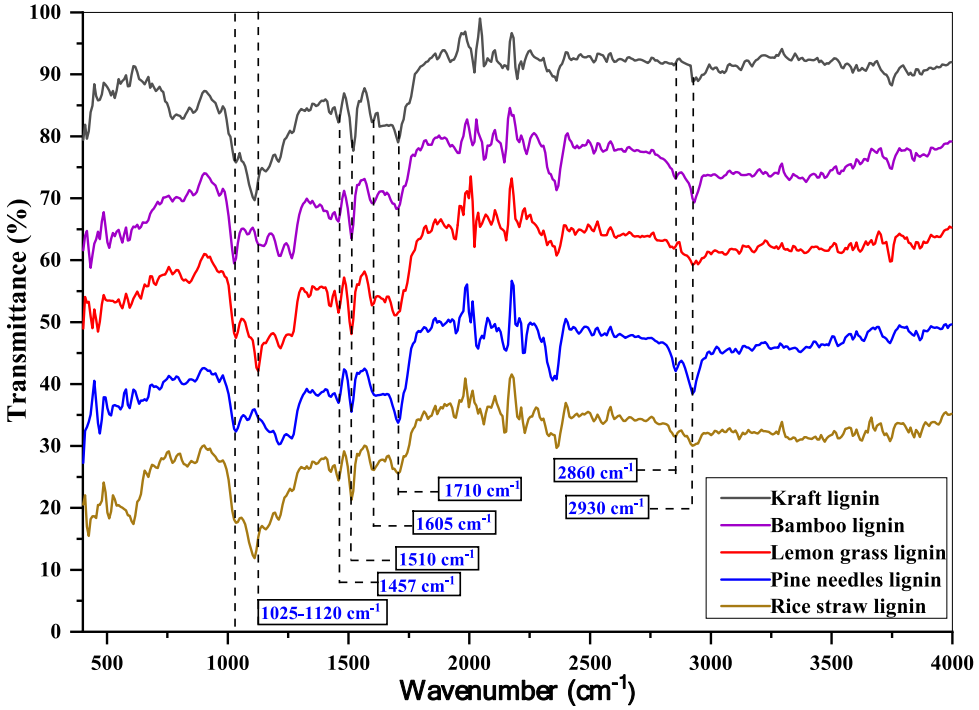

Fig. 2. FTIR spectrum of different biomass-derived lignin.

Also, the porosity analysis of kraft lignin was performed using BET measurements. The results indicate that raw kraft lignin possesses a very low pore volume (0.001099 cc/g), consistent with its non-porous or weakly porous nature (see ESI for more information).

Further, FTIR spectroscopy is a useful analysis technique used to examine the surface structure and characteristic lignin functionalities present in different biomass-derived lignin. As shown in Fig. 2, the FTIR spectrum of kraft lignin and other biomass-derived lignin were almost similar regarding intensity and sharpness of the characteristics peaks lying in 400–4000 cm^{-1} region. The characteristics peak at 1457 cm^{-1} (C—H bending vibration of -CH_2, -CH_3, and C═C stretching vibrations), 1510 and 1605 cm^{-1} (C═C stretching vibrations), and 1710 cm^{-1} resulted in C = 0 stretching vibrations of the aromatic skeletal in different lignin (Yan et al., 2015; Cherif et al., 2020; Yang et al., 2007). Similarly, the peak at 2860 and 2930 cm^{-1} is ascribed to alkane C—H stretching in methyl and methylene groups of aromatic skeletons (Cherif et al., 2020). Other peaks such as in the region of 1025–1120 cm^{-1} existed for aromatic C—H in plane deformation and C—O stretching of guaiacyl and syringyl units of lignin, distinguish the lignin from each other which might influence the yields of desired products (Yang et al., 2007).

3.2. Optimization of reaction conditions

Under this investigation, we began our study by employing kraft lignin as initial feedstock to optimize the reaction conditions for the synthesis of desirable phenolic compounds. In each case, we have performed five parallel reactions of kraft lignin with each reaction containing 200 mg of lignin to make it easier for the quantification of desired products. Initially, we started the reactions of kraft lignin (200 mg) followed by the addition of MnO_2 (0.5 equiv. (w/w), 100 mg) and $Na_2H_3CO_6$ (3 equiv. (w/w), 600 mg) in 3 M NaOH (10 mL) solvent media under hydrothermal reactor at particular reaction time and temperature (Table 1, entry 1). The applied experimental condition resulted in 6, 3, and 1 wt% yields of vanillin (I), vanillic acid (II), and acetovanillone (III). Encouraged by these results, we further screened out the equivalence of MnO_2 and observed that 1 equivalent (w/w) of MnO_2 provided the maximum yields of the desired products (Table 1, entries 2, 3). Similarly, when we optimized the concentration of $Na_2H_3CO_6$ oxidant, it was noticed that enhancing the concentration above 3 equivalents (w/w) had minimal impact on product yields (Table 1, entries 4, 5). In the same fashion, when both MnO_2 and $Na_2H_3CO_6$ were used individually under specified reaction time and temperature, the yields of targeted products drastically reduced (Table 1, entries 6, 7). Therefore, the aforementioned results confirmed that a specific concentration of the reagent system had a synergistic effect in achieving the maximum yields of targeted products. In addition, we have also checked the reaction with H_2O_2 oxidant, which resulted in 5, 3, and 1 wt% yields of vanillin, vanillic acid, and acetovanillone, respectively (Table 1, entry 8). Therefore, $Na_2H_3CO_6$ is the most suitable oxidant under applied reaction conditions. Now, we further optimized the reaction time and temperature to find out the ideal reaction conditions. Through this study, we observed that raising reaction time significantly increased the conversion of lignin and procured satisfactory results at 2 h (Table 1, entries 9, 10, and 2). In the same fashion, the reaction temperature was also optimized which indicated a similar trend in the enhancement of conversion rate with increasing reaction temperature, however, the yields were maximum at 160 °C (Table 1, entries 11, 12, and 2). Hence, the optimized reaction time and temperature for the conversion of lignin to desired products were set to 160 °C and 2 h, respectively. Furthermore, after optimizing the reaction time and temperature, we shifted our attention to the selection of other metal oxides such as Fe_2O_3, CuO, and ZnO. Through this investigation, we found that MnO_2 was the most suitable catalyst for the synthesis of phenolic compounds under established experimental conditions (Table 1, entries 13, 14, and 15). Now, further to examine the influence of NaOH concentration, we performed the reaction with varied molarity of solvent medium and observed that 3 M NaOH concentration of solvent was sufficient for the selective conversion of lignin to acquire good yields of vanillin, vanillic acid, and acetovanillone (Table 1, entries 16 and 17). In addition, we have also performed the reactions using 3 M KOH, water, and MeOH solvent, but only negligible lignin conversion to the targeted phenolic compounds was observed under these conditions (Table 1, entries 18, 19 and 20). Hence, the best optimal reaction

Table 1
Reaction optimization study[a].

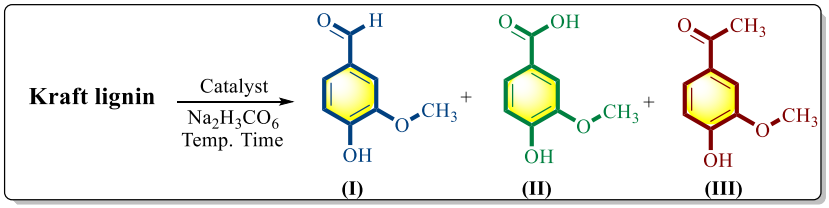

Entry	Catalyst	Time (hrs)	Temperature (°C)	Yield I wt%[b]	Yield II wt%[b]	Yield III wt%[b]
1.[c]	MnO_2	2	160	6	3	1
2.	MnO_2	2	160	8 [10]	5 [6.5]	1.5
3.[d]	MnO_2	2	160	7	5	1.5
4.[e]	MnO_2	2	160	5.5	3.5	1.5
5.[f]	MnO_2	2	160	7	4.5	1.5
6.	–	2	160	3	2	1.5
7.[g]	MnO_2	2	160	2	2	1
8.[h]	MnO_2	2	160	5	3	Traces
9	MnO_2	1	160	5	2	1
10.	MnO_2	3	160	7	5	1
11.	MnO_2	2	140	4	2	1.5
12.	MnO_2	2	180	7	5	1
13.	Fe_2O_3	2	160	5.5	3	2
14.	CuO	2	160	4	3	1
15.	ZnO	2	160	3	1.5	nd
16.[i]	MnO_2	2	160	4	2	nd
17.[j]	MnO_2	2	160	8	4.5	1
18.[k]	MnO_2	2	160	3	3	nd
19.[l]	MnO_2	2	160	nd	nd	nd
20.[m]	MnO_2	2	160	Traces	nd	nd

[a] Reaction condition: kraft lignin (200 mg), MnO_2 (1 equiv. (w/w), 200 mg), $Na_2H_3CO_6$ (3 equiv. (w/w), 600 mg), 3 M NaOH (10 mL).
[b] Wt% yield of products was based on initial weight of kraft lignin.
[c] 0.5 equiv. (w/w) of MnO_2 was used.
[d] 2 equiv. (w/w) of MnO_2 was used.
[e] 2 equiv. (w/w) of $Na_2H_3CO_6$ was used.
[f] 4 equiv. (w/w) of $Na_2H_3CO_6$ was used.
[g] Reaction performed without $Na_2H_3CO_6$.
[h] H_2O_2 was used.
[i] 1 M NaOH solvent used.
[j] 5 M NaOH solvent used.
[k] 3 M KOH solvent used.
[l] Reaction performed in H_2O solvent.
[m] Reaction performed in MeOH solvent. The yields in parentheses represent the total yields of compounds after performing the reactions of precipitated lignin obtained in 1st cycle. All reactions were performed in a hydrothermal reactor system.

conditions for kraft lignin conversion to vanillin (8 ± 0.25 wt%), vanillic acid (5 ± 0.57 wt%), and acetovanillone (1.5 ± 0.39 wt%) were found

Table 2
Synthesis of phenolic compounds from various feedstocks[a].

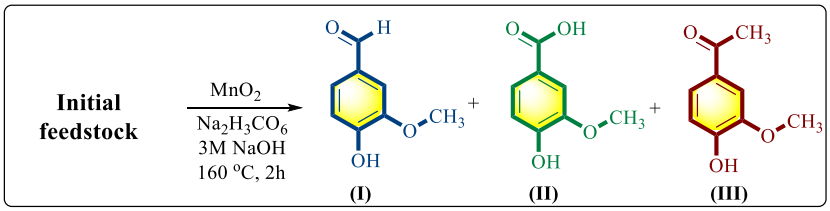

Entry	Initial Feedstock	Yield I wt%[b]	Yield II wt%[b]	Yield III wt%[b]
1	Bamboo lignin	3.5 [5]	3 [4.5]	Traces
2	Lemon grass lignin	6 [8]	3.5 [4.5]	1
3	Pine needles lignin	4 [5.5]	3 [4]	Traces
4	Rice straw lignin	4 [5]	3 [4]	Traces

[a] Reaction condition: Initial feedstock (200 mg), MnO_2 (1 equiv. (w/w), 200 mg), $Na_2H_3CO_6$ (3 equiv. (w/w), 600 mg), 3 M NaOH (10 mL) at 160 °C and 2 h. [b]Wt% yield of products was calculated with respect to the initial weight of lignin. The yields in parentheses represent the total yields of compounds after performing the reactions of precipitated lignin obtained in 1st cycle. All the experimented results are obtained from triplicated assays and the reactions were performed in a hydrothermal reactor system.

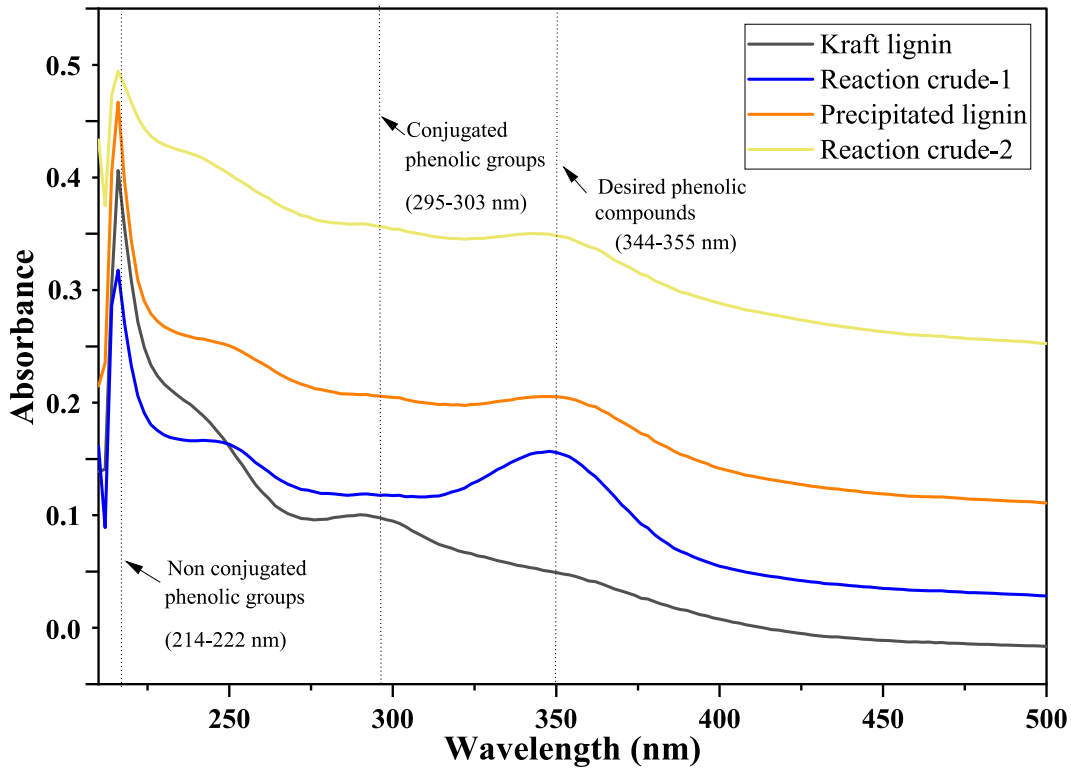

Fig. 3. UV/Vis spectra of a) dissolved kraft lignin b) reaction crude after oxidative depolymerization of kraft lignin c) precipitated lignin d) reaction crude of precipitated lignin.

to be 1 equivalent (w/w) of MnO_2 and 3 equivalent (w/w) of $Na_2H_3CO_6$ in 3 M NaOH (10.0 mL) solvent media at 160 °C temperature for 2 h reaction time.

In addition, after completion of the reaction, the reaction crude was neutralized with 4 N H_2SO_4, resulting in a lowering of the pH and formation of a precipitate of lignin. This precipitated lignin is assumed to be the fractionated portion of lignin and supposed to be enriched with lignin oligomers, which are attractive starting material to further enhance the total yields of phenolic compounds. Therefore, assuming this factor in our mind, we have performed the reaction of precipitated lignin under optimized reaction conditions (see ESI for more information). Surprisingly, we have obtained vanillin and vanillic acid with total yields improved to 10 and 6.5 wt%, respectively, as mentioned in parentheses (Table 1, entry 2).

Furthermore, to extend the applicability of optimized reaction conditions, we have also evaluated the developed protocol on other biomass-derived lignin substrates such as bamboo lignin, lemon grass lignin, pine needles lignin, and rice straw lignin directly to synthesized vanillin, vanillic acid, and acetovanillone. Like kraft lignin, here we performed five parallel reactions of each biomass-derived lignin to simplify the product quantification. Initially, we performed a reaction with bamboo lignin under optimized conditions which resulted in 3.5 and 3 wt% yields of desired compounds (I, II) respectively, although a traces amount of acetovanillone was also observed (Table 2, entry 1). Subsequently, the lemon grass waste derived lignin was directly employed for the production of phenolic compounds with good yields (Table 2, entry 2). In addition, pine needle derived lignin and rice straw-derived lignin were also directly used for the synthesis of vanillin and vanillic acid with satisfactory yields under our set protocol (Table 2, entries 3 and 4). Therefore, the optimized protocol is applicable to various lignin substrates with acceptable yields of desired phenolic compounds. Subsequently, to improve desired compound yields, we further performed the reactions of precipitated lignin under optimized protocols. Therefore, the total yield of products improved as depicted in parentheses (Table 2, entries 1–4). Although, we know that bamboo, lemongrass, pine needle, and rice straw lignins contain syringyl (S), guaiacyl (G), and *p*-hydroxyphenyl (H) units, and the product distribution strongly depends on reaction severity and intermediate stability. In this study, the highly oxidative $MnO_2/Na_2H_3CO_6$ system in hydrothermal conditions resulted in guaiacyl-derived monomers, yielding vanillin, vanillic acid, and acetovanillone as dominant products. In contrast, S- and H-unit-derived compounds were might be formed only transiently and rapidly underwent over-oxidation, demethoxylation, or aromatic ring-opening, preventing their accumulation as stable end products (Rinaldi et al., 2016; Schutyser et al., 2018).

After developing a successful way to depolymerize various biomass-derived lignin to phenolic compounds, we performed UV/Vis spectroscopy to validate our hypothesis with experimental data. The UV/Vis spectra of kraft lignin, reaction crude after completion of the reaction, precipitated lignin, and reaction crude of precipitated lignin are shown in Fig. 3 (samples were referenced by alkaline media). As we can see in the spectra of kraft lignin, it has two shoulder peaks at 214–222 and 296–303 nm of non-conjugated and conjugated phenolic groups, respectively. In literature, these two peaks usually occur at 270–280 and 316–320 nm, however,

owing to the hypsochromic effect of NaOH, the peak absorption is shifted from its actual value (Alzagameem et al., 2018). In addition, the UV spectra of the reaction crude showed a broad absorption at 344–355 nm region, corresponding to desired phenolic compounds (Zirbes et al., 2023). However, the precipitated lignin has a sharp peak at 214–222 nm and a broad peak at 330–378 nm corresponding to non-conjugated and low molecular weight phenolic compounds. Furthermore, the reaction crude of precipitated lignin exhibits a low-intensity shoulder peak, hence it proves the maximum extent of non-conjugated phenolic groups depolymerized into smaller phenolic compounds. Therefore, UV/Vis data of different samples supported our assumption that the precipitated portion of fractionated lignin contains low molecular weight lignin oligomers and can be further converted to desired compounds under our

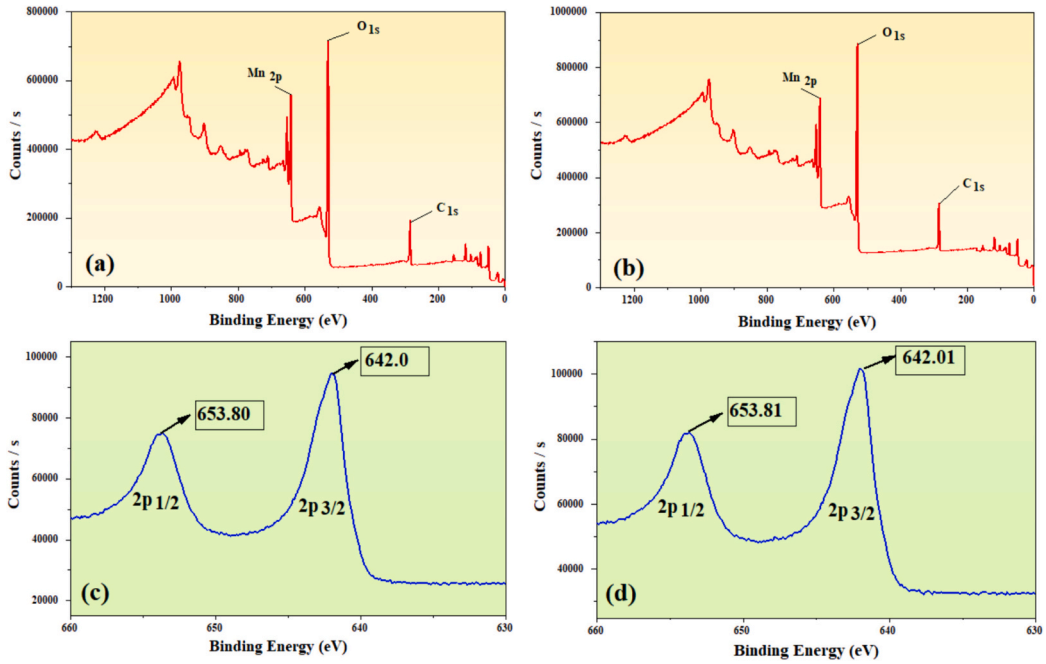

Fig. 4. XPS spectra of MnO_2 (a) fresh, (b) reactivated, and high-resolution Mn 2p core level XPS spectra of MnO_2 (c) fresh, (d) reactivated.

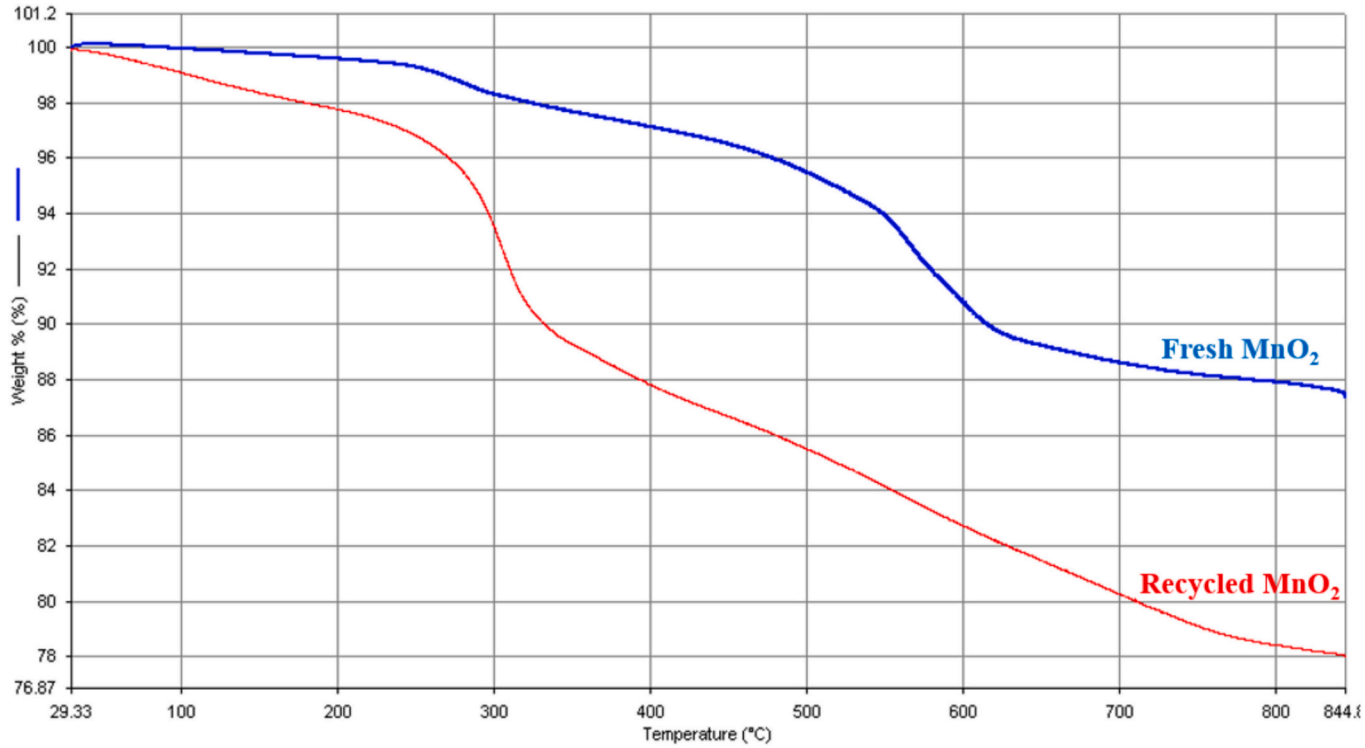

Fig. 5. TGA analysis of fresh and recycled MnO_2.

optimized reaction conditions.

Furthermore, after performing the reaction under optimized conditions, we recovered MnO_2 from the reaction mixture and applied it in the next catalytic cycle. Here, we observed that the recovered MnO_2 resulted in a drastic decrease in the product yields. The deactivation of recovered MnO_2 might be due to the adsorption of lignin or products on the surface of the catalyst inhibiting its oxidation efficiency. However, reactivated MnO_2 provided fruitful conversion of lignin with good yields of products. Further to investigate the oxidation state of fresh and reactivated catalysts, we have performed X-ray photoelectron spectroscopy (XPS) analysis, as shown in Fig. 4. A close inspection of high-resolution Mn2p core level spectra of fresh and reactivated MnO_2 showed two major peaks of Mn exhibited at $2p_{3/2}$ (642.0 eV, 642.01 eV) and $2p_{1/2}$ (653.80 eV, 653.81 eV) respectively (Yu et al., 2021). This study affirmatively supported the +4 oxidation state of fresh and reactivated MnO_2, with a peak splitting difference of 11.8 eV. Additionally, we performed thermogravimetric analysis (TGA) to evaluate the thermal stability and structural integrity of both fresh and recycled MnO_2 catalysts, as shown

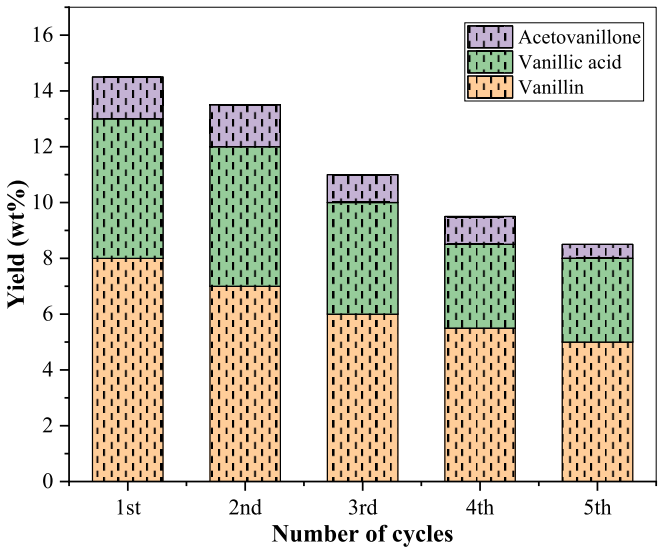

Fig. 6. Recyclability test.

in Fig. 5. The TGA profiles reveal distinct weight-loss behaviors, indicating changes in surface chemistry and catalyst composition after catalytic recycling. As we can see in the TGA graph, the fresh MnO_2 exhibits minimal weight loss below.

150 °C due to the removal of adsorbed moisture and shows a total mass loss of ~12–13 wt% up to 840 °C, indicating good thermal stability. In contrast, the recycled MnO_2 shows a higher and continuous weight loss, particularly in the 250–350 °C range, which is attributed to the decomposition of surface-deposited lignin residues, followed by additional mass loss at higher temperatures due to partial reduction of MnO_2, resulting in ~78 wt% residue at 840 °C. In addition, once the methodology was critically optimized for the procurement of satisfied yields of vanillin, vanillic acid, and acetovanillone, then we performed a recyclability test of MnO_2 by using kraft lignin as the initial substrate under optimized standard reaction conditions. After the reaction was completed, the product was recovered from the reaction mixture using a simple filtration method and then washed with methanol to dissolve any residual lignin. After that, it was again washed with acetone 3 to 4 times and further dried in a rotary evaporator. The dried MnO_2 was activated in a high-pressure autoclave reactor at 230 °C and 10 bar oxygen pressure for 2 h. However, when recycled or washed, MnO_2 was directly employed in the next consecutive cycle without any activation, we observed a light spot of products on TLC. From all these results, we found that the MnO_2 shows remarkable activity for lignin depolymerization to desired products up to 5 cycles with a slight decrease in product yields. However, the decrease in product yields after the 5th cycle (Fig. 6) might be due to the combination of several factors, such as partial reduction of Mn^{4+} with incomplete re-oxidation, structural changes or phase transformation under hydrothermal conditions, and adsorption of lignin or products on the surface of the catalyst. These effects reduce the number of accessible active sites, limiting catalyst recyclability despite oxygen reactivation under high pressure. In addition, we have also performed FTIR analysis of fresh and recycled catalyst and observed that the FTIR spectrum of recycled MnO_2 shows noticeable changes in the Mn—O bending vibration around ~452 cm^{-1} compared to fresh MnO_2 (see ESI for more information). This band is associated with O-Mn-O deformation modes (Julien et al., 2004). The reduced intensity and slight broadening of this peak after recycling suggest lattice distortion and modification of the surface coordination environment, likely arising through oxygen vacancy formation during catalytic oxidation.

Based on the previous literature reports, we also discussed the best plausible mechanistic consideration for the depolymerization of lignin to vanillin, vanillic acid, and acetovanillone. As we know, lignin consists of different types of C—O ether /C-C linkages, and the breaking of C—C bonds results in the formation of vanillin; however, the cleavage of C—O ether linkages with keto-enol isomerization could be responsible for the formation of acetosyringone (Kumar et al., 2022). In the plausible reaction mechanism, $Na_2H_3CO_6$ decomposes to generate hydrogen peroxide (H_2O_2) and other reactive oxygen species, while MnO_2 (Mn^{4+}) facilitates radical formation. The synergistic interaction between $Na_2H_3CO_6$ and MnO_2 promotes the continuous in situ generation of hydroxyl (·OH) and superoxide ($O_2{\cdot}^-$) radicals, thereby maintaining a highly oxidative reaction environment (Sun et al., 2020). The ·OH radicals abstract hydrogen atoms from benzylic Cα-H bonds, phenolic -OH groups, and aliphatic side chains within β-O-4 lignin linkages, resulting in the formation of phenoxy and benzylic lignin-centered radicals. These radicals subsequently react with $O_2{\cdot}^-$ to form peroxy intermediates, which undergo Cα-Cβ bond and β-O-4 ether bond cleavage (Sun et al., 2020; Norberg et al., 2025). This oxidative fragmentation yields guaiacyl-derived aromatic monomers, including vanillin, vanillic acid, and acetovanillone (Tang et al., 2024; Norberg et al., 2025). Thus, the combined effect of both MnO_2 and sodium percarbonate help in depolymerization of lignin to desired phenolic compounds. Also, it has been noticed that the reaction does not take place without alkaline NaOH solvent media, and the alkaline reaction conditions are most favorable

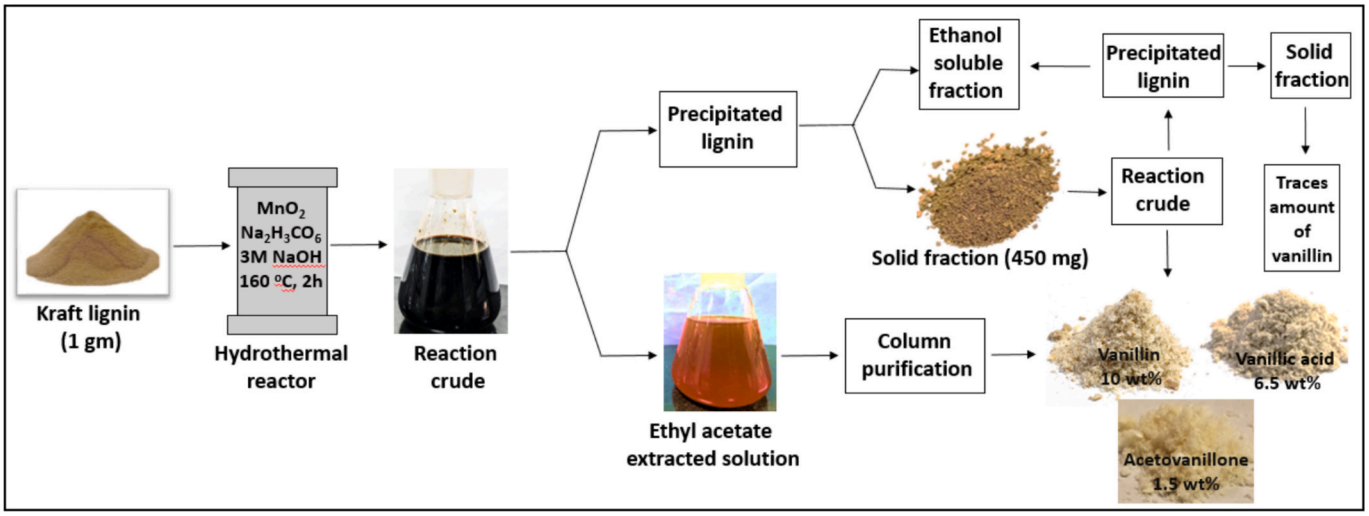

Fig. 7. Schematic representation of kraft lignin depolymerization to phenolic compounds.

for the efficient deprotonation of the substrates to enhance phenolic compound synthesis (Zhang et al., 2020). In addition, we have also proposed a schematic diagram for the kraft lignin oxidative depolymerization setup as shown in Fig. 7. Furthermore, the ethanol-soluble part may contain a low molecular weight fraction that has promising applications in the petrochemicals industry, and further work is still ongoing in our next phase research.

4. Conclusion

In summary, we have demonstrated a MnO_2 and sodium percarbonate mediated reagent system for the depolymerization of commercially available kraft lignin and biomass-derived lignin from bamboo, lemongrass, pine needles, and rice straw in alkaline solvent media to vanillin, vanillic acid, and acetovanillone with 3.5–10, 3–6.5, 1–1.5 wt% yields respectively under a pressurized hydrothermal reactor system. The SEM and FTIR analysis were also performed to find out the morphological variations, particle size distribution, and the characteristics functionalities of different lignin substrates. Moreover, the heterogeneous MnO_2 was easily recyclable up to five cycles and the comprehensive characterization of fresh and reactivated MnO_2 was analyzed by XPS technique, and the loss of recycled MnO_2 activity has been confirmed through TGA analysis. However, the amount of MnO_2 and sodium percarbonate for the depolymerization of lignin is still high, and in the future, further study is required to improve the catalytic efficiency of MnO_2 for complete fractionation of lignin resulting in excellent yields of phenolic compounds.

CRediT authorship contribution statement

Rohit Bains: Writing – original draft, Methodology, Investigation, Formal analysis, Conceptualization. **Mahender Kumar:** Investigation, Data curation. **Arvind Singh Chauhan:** Investigation, Data curation. **Ajay Kumar:** Data curation. **Pralay Das:** Writing – review & editing, Supervision.

Declaration of competing interest

The authors declare that they have no known competing financial interests or personal relationships that could have appeared to influence the work reported in this paper.

Acknowledgements

We are grateful to the Director of CSIR-IHBT for providing the necessary facilities during the course of this work. The authors thank CSIR, New Delhi, for financial support as part of project numbers HCP-0007 and MLP-0203. We also thank AMRC and IIT Mandi for XPS analysis. RB, MK, ASC, and AK thank CSIR and DST-INSPIRE, New Delhi, for awarding fellowships. #CSIR-IHBT communication No. 5598.

Appendix A. Supplementary data

Supplementary data to this article can be found online at https://doi.org/10.1016/j.biteb.2026.102676.

Data availability

The data that support the findings of this study are available in the supplementary material of the article.

References

Alzagameem, A., Hansen, B.E.K.-., Büchner, D., Larkins, M., Kamm, B., Witzleben, S., Schulze, M., 2018. Lignocellulosic biomass as source for lignin-based environmentally benign antioxidants. Molecules 23, 2664. https://doi.org/10.3390/molecules23102664.

Bains, R., Kumar, A., Chauhan, A.S., Das, P., 2022. Dimethyl carbonate solvent assisted efficient conversion of lignocellulosic biomass to 5- hydroxymethylfurfural and furfural. Renew. Energy 197, 237–243. https://doi.org/10.1016/j.renene.2022.07.076.

Bains, R., Chauhan, A.S., Kumar, A., Kumar, M., Das, P., 2024. 5-Hydroxymethylfurfural and furfural synthesis from waste paper, cotton and poly/mono-meric carbohydrates. Biomass Bioenergy 188, 107314. https://doi.org/10.1016/j.biombioe.2024.107314.

Bajwa, D.S., Pourhashem, G., Ullah, A.H., Bajwa, S.G., 2019. Concise review of current lignin production, applications, products and their environment impact. Ind. Crop. Prod. 139, 11152. https://doi.org/10.1016/j.indcrop.2019.111526.

Banu, J.R., Preethi, Kavitha, S., Tyagi, V.K., Gunasekaran, M., Karthikeyan, O.P., Kumar, G., 2021. Lignocellulosic biomass based biorefinery: a successful platform towards circular bioeconomy. Fuel 302, 121086. https://doi.org/10.1016/j.fuel.2021.121086.

Bu, Q., Lei, H., Zacher, A.H., Wang, L., Ren, S., Liang, J., Wei, Y., Liu, Y., Tang, J., Zhang, Q., Ruan, R., 2012. A review of catalytic hydrodeoxygenation of lignin-derived phenols from biomass pyrolysis. Bioresour. Technol. 124, 470–477. https://doi.org/10.1016/j.biortech.2012.08.089.

Cao, Y., Chen, S.S., Zhang, S., Ok, Y.S., Matsagar, B.M., Wu, K.C.-W., Tsang, D.C.W., 2019. Advances in lignin valorization towards bio-based chemicals and fuels: Lignin biorefinery. Bioresour. Technol. 291, 121878. https://doi.org/10.1016/j.biortech.2019.121878.

Cherif, M.F., Trache, D., Brosse, N., Benaliouche, F., Tarchoun, A.F., 2020. Comparison of the physicochemical properties and thermal stability of organosolv and kraft lignins from hardwood and softwood biomass for their potential valorization. Waste Biomass Valoriz. 11, 6541–6553. https://doi.org/10.1007/s12649-020-00955-0.

Deng, H., Lin, L., Sun, Y., Pang, C., Zhuang, J., Ouyang, P., Li, J., Liu, S., 2009. Activity and stability of perovskite-type oxide $LaCoO_3$ catalyst in lignin catalytic wet oxidation to aromatic aldehydes process. Energy Fuel 23, 19–24. https://doi.org/10.1021/ef8005349.

Fache, M., Boutevin, B., Caillol, S., 2015. Vanillin, a key-intermediate of biobased polymers. Eur. Polym. J. 68, 488–502. https://doi.org/10.1016/j.eurpolymj.2015.03.050.

Gillet, S., Aguedo, M., Petitjean, L., Morais, A.R.C., da Costa Lopes, A.M., Lukasik, R.M., Anastas, P.T., 2017. Lignin transformations for high value applications: towards targeted modifications using green chemistry. Green Chem. 19, 4200–4233. https://doi.org/10.1039/C7GC01479A.

Harshvardhan, K., Suri, M., Goswami, A., Goswami, T., 2017. Biological approach for the production of vanillin from lignocellulosic biomass (Bambusa tulda). J. Clean. Prod. 149, 485–490. https://doi.org/10.1016/j.jclepro.2017.02.125.

Julien, C.M., Massot, M., Poinsignon, C., 2004. Lattice vibrations of manganese oxides: part I. Periodic structures. Spectrochim. Acta Part A 60, 689–700. https://doi.org/10.1016/S1386-1425(03)00279-8.

Kaur, J., Gulati, M., Singh, S.K., Kuppusamy, G., Kapoor, B., Mishra, V., Gupta, S., Arshad, M.F., Porwal, O., Jha, N.K., Chaitanya, M.V.N.L., Chellappan, D.K., Gupt, G., Gupta, P.K., Dua, K., Khursheed, R., Awasthi, A., Corrie, L., 2022. Discovering multifaceted role of vanillic acid beyond flavours: nutraceutical and therapeutic potential. Trends Food Sci. Technol. 122, 187–200. https://doi.org/10.1016/j.tifs.2022.02.023.

Kumar, A., Biswas, B., Saini, K., Kumar, A., Kumar, J., Krishna, B.B., Bhaskar, T., 2022. Copper and manganese bimetallic catalysts for oxidation of prot lignin: effects of metal oxide on product yield. Biomass Convers. Biorefinery 12, 115–128. https://doi.org/10.1007/s13399-020-01167-1.

Kumar, A., Chauhan, A.S., Bains, R., Das, P., 2023. Catalytic transformations for agro-waste conversion to 5-hydroxymethylfurfural and furfural: Chemistry and scale-up development. Green Chem. 25, 849–870. https://doi.org/10.1039/D2GC03999K.

Li, C., Zhao, X., Wang, A., Huber, G.W., Zhang, T., 2015. Catalytic transformation of lignin for the production of chemicals and fuels. Chem. Rev. 115, 11559–11624. https://doi.org/10.1021/acs.chemrev.5b00155.

Liu, S., Shi, Z., Li, L., Yu, S., Xiec, C., Songa, Z., 2013. Process of lignin oxidation in an ionic liquid coupled with separation. RSC Adv. 3, 5789–5793. https://doi.org/10.1039/C3RA40391B.

Liu, S., Das, L., Blauch, D.N., Veronee, C., Dou, C., Gladden, J., Sun, N., Socha, A.M., 2020. Statistical design of experiments for production and purification of vanillin and aminophenols from commercial lignin. Green Chem. 22, 3917–3926. https://doi.org/10.1039/D0GC01234C.

Norberg, M., Bekirovska, S., Klein, J., Moeller, F., Gustafson, K.P.J., Sandahl, M., Hulteberg, C.P., Turner, C., Abdelaziz, O.Y., Waldvogel, S.R., Spegel, P., Bengtsson, O., 2025. Oxidative depolymerization of lignosulfonates to low-molecular weight aromatics: an interlaboratory study. RSC Sustain. 3, 4818–4824. https://doi.org/10.1039/D5SU00698H.

Pacek, A.W., Ding, P., Garrett, M., Sheldrake, G., Nienow, A.W., 2013. Catalytic conversion of sodium lignosulfonate to vanillin: engineering aspects. Part 1. Effects of processing conditions on vanillin yield and selectivity. Ind. Eng. Chem. Res. 52, 8361–8372. https://doi.org/10.1021/ie4007744.

Rinaldi, R., Jastrzebski, R., Clough, M.T., Ralph, J., Kennema, M., Bruijnincx, P.C.A., Weckhuysen, B.M., 2016. Paving the way for lignin valorisation: recent advances in bioengineering, biorefining and catalysis. Angew. Chem. Int. Ed. 55, 8164–8215. https://doi.org/10.1002/anie.201510351.

Schutyser, W., Renders, T., Bosch, S.V.-den., Koelewijn, S.-F., Beckham, G.T., Sels, B.F., 2018. Chemicals from lignin: an interplay of lignocellulose fractionation, depolymerisation, and upgrading. Chem. Soc. Rev. 47, 852–908. https://doi.org/10.1039/C7CS00566K.

Stark, K., Taccardi, N., Bosmann, A., Wasserscheid, P., 2010. Oxidative depolymerization of lignin in ionic liquids. ChemSusChem 3, 719–723. https://doi.org/10.1002/cssc.200900242.

Stefanska, J., Pawliczak, R., 2008. Apocynin: molecular aptitudes. Mediat. Inflamm. 2008, 106507. https://doi.org/10.1155/2008/106507.

Sun, Z., Fridrich, B., de Santi, A., Elangovan, S., Barta, K., 2018. Bright side of lignin depolymerization: toward new platform chemicals. Chem. Rev. 118, 614–678. https://doi.org/10.1021/acs.chemrev.7b00588.

Sun, S., Akiyama, T., Yokoyama, T., Matsumoto, Y., 2020. Differences in the mechanisms of MnO2 oxidation between lignin model compounds with the p-hydroxyphenyl, guaiacyl, and syringyl nuclei. J. Agric. Food Chem. 68, 6819–6825. https://doi.org/10.1021/acs.jafc.0c01956.

Tang, C., Cao, Y., Gao, J., Luo, G., Fan, J., Clark, J.H., Zhang, S., 2024. Oxidative catalytic depolymerization of lignin into value-added monophenols by carbon nanotube-supported Cu-based catalysts. Molecules 29, 4762. https://doi.org/10.3390/molecules29194762.

Voitl, T., Roh, P.R., 2010. Demonstration of a process for the conversion of kraft lignin into vanillin and methyl vanillate by acidic oxidation in aqueous methanol. Ind. Eng. Chem. Res. 49, 520–525. https://doi.org/10.1021/ie901293p.

Walch, F., Abdelaziz, O.Y., Meier, S., Bjelic, S., Hulteberg, C.P., Riisager, A., 2021. Oxidative depolymerization of Kraft lignin to high-value aromatics using a homogeneous vanadium–copper catalyst. Catal. Sci. Technol. 11, 1843–1853. https://doi.org/10.1039/D0CY02158J.

Yamamoto, K., Hosoya, T., Yoshioka, K., Miyafuji, H., Ohno, H., Yamada, T., 2017. Tetrabutylammonium hydroxide 30-hydrate as novel reaction medium for lignin conversion. ACS Sustain. Chem. Eng. 5, 10111–10115. https://doi.org/10.1021/acssuschemeng.7b02106.

Yan, P., Xu, Z., Zhang, C., Liu, X., Xua, W., Zhang, Z.C., 2015. Fractionation of lignin from eucalyptus bark using amine-sulfonate functionalized ionic liquids. Green Chem. 17, 4913–4920. https://doi.org/10.1039/C5GC01035G.

Yang, H., Yan, R., Chen, H., Ho Lee, D., Zheng, C., 2007. Characteristics of hemicellulose, cellulose and lignin pyrolysis. Fuel 86, 1781–1788.

Yu, L., Mo, Z., Zhu, X., Deng, J., Xu, F., Song, Y., She, Y., Li, H., Xu, H., 2021. Construction of 2D/2D Z-scheme MnO_2-x/g-C3N4 photocatalyst for efficient nitrogen fixation to ammonia. Green Energy Environ. 6, 538–545. https://doi.org/10.1016/j.gee.2020.05.011.

Zhang, R., Maltari, R., Guo, M., Kontro, J., Eronen, A., Repo, T., 2020. Facile synthesis of vanillin from fractionated Kraft lignin. Ind. Crop. Prod. 145, 112095. https://doi.org/10.1016/j.indcrop.2020.112095.

Zirbes, M., Graßl, T., Neuber, R., Waldvogel, S.R., 2023. Peroxodicarbonate as a green oxidizer for the selective degradation of kraft lignin into vanillin. Angew. Chem. Int. Ed. 62, e202219217. https://doi.org/10.1002/anie.202219217.